MOLECULAR PHYSICS, 1984, VOL. 52, NO. 6, 1303–1334

Monte Carlo study of the isotropic and nematic phases of infinitely thin hard platelets

by R. EPPENGA† and D. FRENKEL
Fysisch Laboratorium, Rijksuniversiteit Utrecht,
P.O. Box 80000, 3508 TA Utrecht, The Netherlands

(*Received* 11 *November* 1983 ; *accepted* 21 *March* 1984)

We present the results of a detailed Monte Carlo study of the phase diagram of infinitely thin hard platelets. A weak first order isotropic-nematic transition is observed. The equation of state in the isotropic regime is compared with several current theories, none of which is found to be fully satisfactory. The density dependence of the nematic order parameter is found to be compatible with a ' critical ' exponent $\beta = 0{\cdot}25$. A study of the fluctuations of the order parameter in the isotropic phase casts doubt on the applicability of the Landau-de Gennes expression for the free energy. We observe that the relation between the nematic order parameters $\langle P_2 \rangle$ and $\langle P_4 \rangle$ is compatible with the predictions of mean-field theory. Practical aspects of the computation are discussed. A novel method to compute the pressure in a constant-volume Monte Carlo run is presented.

1. INTRODUCTION

In this paper we present results of a computer simulation study of a simple model system which has both an isotropic and a nematic phase. The model fluid under consideration consists of infinitely thin hard platelets of diameter σ (figure 1). Apart from its sheer simplicity this system has a number of attractive features which make it a suitable candidate for a systematic numerical study. The present article is organized as follows : first we discuss the incentive for carrying out a computer simulation study of the hard-platelets system. Next we elaborate on some non-standard aspects of the computational method used. Finally we present the results of the computer simulations and discuss their implications for existing theories of the nematic phase and the nematic–isotropic phase transition.

Many molecular fluids consisting of anisometric molecules exhibit one or several liquid crystalline phases between the usual isotropic liquid phase and the solid phase [1]. Simplest among these liquid crystalline phases is the nematic phase which is characterized by short range translational, and long range orientational order. Whether or not a given molecular liquid will have a nematic phase depends in a rather subtle way on the shape of the constituent molecules. First of all the intermolecular interactions have to be sufficiently anisotropic to favour orientational ordering. However, most non-spherical molecules freeze before they can form a liquid crystal. Therefore a good model for a nematogen must satisfy two conditions (1) it must be sufficiently anisotropic to favour orientational

† Present address : Philips Research Laboratories, Eindhoven, The Netherlands.

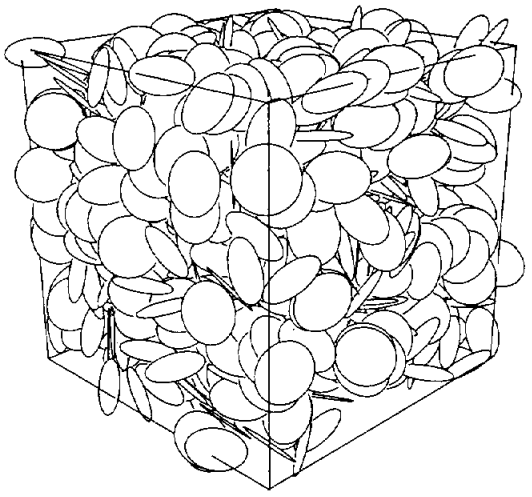

Figure 1. Snapshot of a typical configuration of an 800 particle hard-platelet fluid at a density $No^3/V = 3{\cdot}75$, i.e. just below the isotropic–nematic transition.

order and (2) at the temperature and density of the isotropic–nematic transition the solid phase should still be thermodynamically unstable. Two distinct molecular properties may help to favour the nematic phase over the solid. The first is the presence of internal degrees of freedom which contribute to the entropy in the liquid phase but are frozen out in the solid. Most thermotropic liquid crystal belong to this category. The second possibility is that the average excluded volume of a pair of randomly oriented molecules is much larger than the volume occupied by these molecules in a close packed crystal. In this case the density at which orientational ordering becomes favourable is much lower than the freezing density. Many lyotropic liquid crystals fit this description. Most models for nematic ordering either belong to the latter category (the Onsager theory [2] is the outstanding example) or ignore the possibility of freezing altogether (this is true for the Maier–Saupe theory [3] as well as for many of the applications of scaled particle theory [4, 5]). The model system discussed in the present paper cannot crystallize at any finite density because infinitely thin discs have zero volume. Yet as two non-parallel discs have a finite excluded volume, orientational ordering can, and in fact must, occur at a finite density. We therefore expect the hard-platelet system to exhibit an isotropic phase at low densities and a nematic phase at high densities. No other phases of the hard-platelet system are to be expected. It is for this reason that hard-platelets constitute a very ' clean ' model system to study the isotropic–nematic transition. There are several questions related to the isotropic–nematic transition which make a numerical study of this model system interesting. The first question is related to the role of repulsive forces in driving the I–N transition. Whereas there is general consensus that the structure of simple liquids is almost exclusively determined by the strong repulsive forces that act between atoms at short distances (see, e.g. [6]), the situation is less clear in the case of liquid crystals. There are two distinct theoretical approaches to the description of the I–N

transition based on almost diametrically opposed points of view. On the one hand there is the Maier–Saupe (M–S) theory, a mean-field description which never considers the effect of harsh repulsive forces on the liquid structure explicitly. In the M–S theory the onset of nematic ordering is attributed to the effect of relatively long-ranged anisotropic intermolecular interactions (e.g. the anisotropic dispersion forces which decay as r^{-6}). The M–S theory yields a qualitatively correct description of a number of properties of nematic liquid crystals (see, e.g. [7]), but the assumption that harsh repulsive forces are irrelevant is hard to justify. However, it was recently pointed out by Sluckin and Shukla [8] that the main results of the M–S theory can be rederived without such an assumption, but at a cost : the simple relation between ' molecular field ' and intermolecular potential is replaced by a much more complicated one. On the other hand there are several theoretical approaches which start out from the assumption that the effect of the anisotropic repulsive forces on the liquid structure is of crucial importance for the transition to the nematic phase. Oldest among these is Onsager's theory for the I–N transition of a system of thin hard rods [2]. The Onsager theory predicts that such a system will exhibit a very strong first order isotropic–nematic transition ($\Delta\rho/\rho \sim 26$ per cent). This may be correct for thin rods but it is certainly of little relevance for typical thermotropic liquid crystals which have a very weak I–N transition ($\Delta\rho/\rho < 1$ per cent). Scaled particle theories [4, 5] seem somewhat better suited to describe the onset of nematic ordering in fluids of harshly repulsive particles with realistic length-to-width ratios. There is, however, a conspicuous scarcity of numerical data on the equation of state of hard, non-spherical convex bodies to which the scaled particle predictions can be compared.

In the few cases where a direct comparison has been made [9, 10] the predictions of scaled particle theory are found to deviate by at most 20 per cent (and often much less) from the numerical data.

It is for this reason that we felt that there was a great need for numerical data on a simple hard-core model system which exhibits an isotropic–nematic transition. Such a simulation could be used to test existing theories for the I–N transition in fluids of hard anisometric molecules.

In particular, it could shed some light on the question whether some of the problems with hard-particle theories for the I–N transition (e.g. their consistent overestimation of the volume change at the I–N transition) are due to deficiencies of the model or rather to the approximate nature of the theories used. A complementary question that we will also touch upon is to what extent the applicability of the Maier–Saupe theory is limited to fluids with long-range anisotropic intermolecular interactions. Finally we will also discuss the validity of the purely phenomenological, Landau–de Gennes theory for the isotropic–nematic (I–N) phase transition (see [1]) in the light of the simulation results.

2. Computational method

2.1. *General aspects*

In this section we discuss the numerical method used to obtain the equation of state of the hard platelet system. In particular, we describe in some detail those aspects of the computation that are either peculiar to this system, or more general but non-standard.

For most of our simulations we used the constant-pressure Monte Carlo method [11, 12] on systems of N particles, with $N=25$, 50, 100, 400 and 800. Most runs were done for the $N=100$ system. In all cases cubic periodic boundary conditions were employed. The chemical potential of the platelets was obtained using Widom's particle insertion method [13, 14].

In § 2.3 we describe a simple method to improve the statistics of the particle insertions method in the nematic phase. For some computations it was useful to have the volume rather than the pressure as independent variable. In § 2.4 we present an efficient method to evaluate the pressure in such constant volume runs. We also devote a section (2.5) to the numerical evaluations of the nematic order parameter and its distribution. First, however, we describe the core of the Monte Carlo program, i.e. the part that takes care of random particle displacements and volume changes.

2.2. *Monte Carlo moves*

The first step in starting a series of Monte Carlo runs is the preparation of an acceptable initial configuration. In the present simulations the initial configuration was such that all platelets were aligned but with their centres of mass distributed randomly over the cubic box. Subsequent runs were usually started from previously equilibrated configurations at higher or lower pressures.

The basic Monte Carlo move consisted of a combined random translation and rotation of one particle at a time. The attempted translational displacement $\Delta\mathbf{r}$ was such that Δx, Δy and Δz where random numbers in the interval $[(-\Delta/2), (\Delta/2)]$ with Δ chosen such that a reasonable overall acceptance (typically ~ 30 per cent) was achieved. The random orientational displacements of the unit vector characterizing the molecular orientation had to satisfy two important conditions, the first being that the average size of the displacement was independent of the instantaneous molecular orientation, the second that repeated application of the random reorientation process on an isolated molecule would result in a isotropic distribution of the molecular orientation over the unit sphere. In practice we achieved this by adding a vector $\mathbf{l}$ of fixed length but random orientation to the unit vector characterizing the molecular orientation: $\mathbf{l}=l((1-R_1^2)^{1/2}\cos(2\pi R_2), (1-R_1^2)^{1/2}\sin(2\pi R_2), R_1)$, where R_1 and R_2 are uniformly distributed random numbers, $-1<R_1<+1$ and $0<R_2<1$. The length of $\mathbf{l}$ was chosen such that the overall acceptance of particle moves was about half of what it would be with $l=0$. After normalizing the resulting vector we obtain a unit vector which specifies the attempted molecular orientation. An attempted particle move is accepted if the moved platelet does not intersect any other platelets in its new position. As the test whether two particles intersect is the most frequent operation in the program it is worthwhile to make it computationally cheap.

The test proceeds in four steps:

(1) test if the distance between particles i and j ($|\mathbf{r}_{ij}|$) is less than σ. If not, the platelets cannot intersect (see figure 2);

(2) test if platelet i intersects the plane of platelet j (figure 2 (a)); and

(3) conversely if platelet j intersects the plane of i (figure 2 (b)). If either condition is not met i and j cannot intersect. To perform tests (2) and (3) one needs to know the distance of the centre of $i(j)$ to the intersection

of the planes through platelets i and j. This distance is given by:

$$a_i^2=(\mathbf{r}_{ij}\,.\,\mathbf{n}_j)^2/(1-(\mathbf{n}_i\,.\,\mathbf{n}_j)^2) \quad \text{for particle } i$$

and

$$a_j^2=(\mathbf{r}_{ij}\,.\,\mathbf{n}_i)^2/(1-(\mathbf{n}_i\,.\,\mathbf{n}_j)^2) \quad \text{for particle } j$$

where $\mathbf{n}_i(\mathbf{n}_j)$ is a unit vector perpendicular to the plane through platelet $i(j)$. If particle i intersects the plane of j, $a_i^2<(\sigma/2)^2$. The same condition should hold for a_j^2.

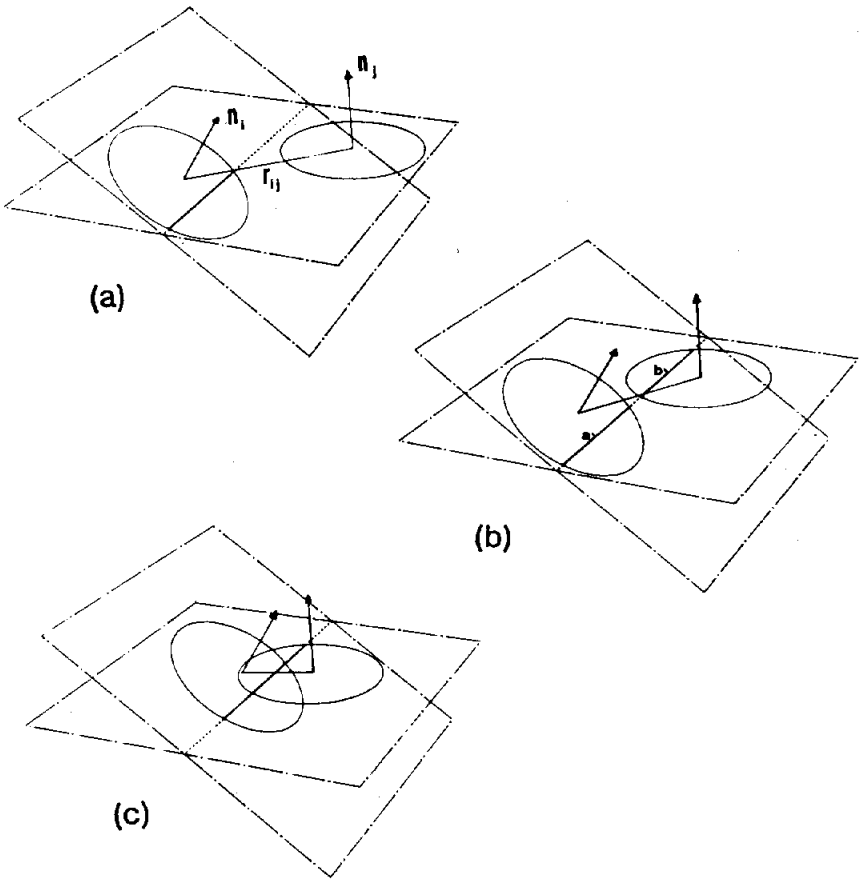

Figure 2. Stages in the test for overlap of two thin hard platelets (see text). (*a*) One particle intersects the plane of the other, but not conversely. (*b*) Both particles intersect the plane of the other, but the platelets do not intersect. (*c*) Inequality 1 (see text) is satisfied, hence the two platelets intersect.

If all of the above conditions are met we still have to check whether platelets i and j physically intersect (see figure 2). This condition is most easily expressed as follows:

(4) The plane of j intersects platelet i over a line segment of length $2\Delta_i$ (with $\Delta_i^2=(\sigma/2)^2-a_i^2$), similarly the plane of i intersects platelet j over a line segment of length $2\Delta_j$ (with $\Delta_j^2=(\sigma/2)^2-a_j^2$). Platelets i and j

intersect if the distance between the middle of these two line segments ($s = |\mathbf{r}_{ij} \cdot \mathbf{n}_i \wedge \mathbf{n}_j)|/(|\mathbf{n}_i \wedge \mathbf{n}_j|$) is less than $\Delta_i + \Delta_j$.

This test can be written in a form that is more suitable for computation, namely :

$$\left(\frac{r_i^2}{2} - \left(\frac{\sigma}{2}\right)^2\right) \sin^2 \theta_{ij} + (\mathbf{r}_{ij} \cdot \mathbf{n}_j)(\mathbf{n}_i \cdot \mathbf{n}_j)(\mathbf{n}_j \cdot \mathbf{r}_{ij})$$
$$< [((\sigma/2)^2 \sin^2 \theta_{ij} - (\mathbf{r}_{ij} \cdot \mathbf{n}_i)^2)((\sigma/2)^2 \sin^2 \theta_{ij} - (\mathbf{r}_{ij} \cdot \mathbf{n}_j)^2)]^{1/2}. \quad (1)$$

In practice we test this inequality without evaluating a single square root by first testing whether the left hand side of (1) is negative (in which case the platelets intersect). If not, we test if the square of the left hand side is smaller than the square of the right hand side. In practice, these tests can be carried out quite efficiently.

The constant-pressure Monte Carlo method is similar to the conventional constant volume Monte Carlo but for the fact that a random volume change is a legitimate Monte Carlo move (14). Whether or not such a move is accepted depends on the change in the value of the weighting function w :

$$w \simeq c \frac{V^N}{N!} \exp [-\beta(U(q^N) + PV)] \quad (2)$$

if V is changed by an amount ΔV, then $r = w_{\mathrm{NEW}}/w_{\mathrm{OLD}}$ is given by :

$$r = \exp [-\beta(\Delta U + P\Delta V - NkT \ln ((V + \Delta V))/V))] \quad (3)$$

if $r \geqslant 1$ the move is accepted ; if $0 < r < 1$, r is compared with a random number $0 < x < 1$. The move is accepted if $x \leqslant r$. It is important that the random moves ΔV be chosen such that any Markov chain in V is reversible. In our computation we found it more convenient to perform a reversible random walk in $\ln V$ rather than in V itself, because the domain of the random walk in $\ln V$ coincides with the range of acceptable (positive) values of V. Moreover, the average stepsize in $\ln V$ is much less density-dependent than the stepsize in V. As a consequence the weighting function changes to w' :

$$w' = c \frac{V^{N+1}}{N!} \exp [-\beta(U(q^N) + PV)]. \quad (4)$$

This may seem a minor point, but it is important that a weighting function consistent with the type of random walk be used.

2.3. *Chemical potential*

The chemical potential per particle in a one-component system is given by :

$$\mu = \left(\frac{\partial G}{\partial N}\right)_{P,T} = \left(\frac{\partial A}{\partial N}\right)_{V,T}. \quad (5)$$

Widom has shown [13] that the chemical potential is related to the probability of acceptance of a Monte Carlo move in which a particle is added at random to an N-particle system :

$$\mu_{\mathrm{EX}} = -kT \ln \langle P_{\mathrm{Acc}} \rangle \quad (6)$$

where μ_{EX} is the excess chemical potential, i.e. the difference between the chemical potential of the fluid at density ρ and an ideal gas at the same density.

For all hard core systems studied thus far $\langle P_{\text{Acc}}\rangle$, the average probability of acceptance becomes vanishingly small at typical liquid densities. However, as the molecules of the hard platelet system have zero volume, the probability of accepting an extra particle remains measurable even at quite high densities and Widom's method can be used to determine the chemical potential of the nematic and isotropic phases at the phase transition. Thus even at the I–N transition $\langle P_{\text{Acc}}\rangle > 2\times 10^{-3}$; this should be compared with $\langle P_{\text{Acc}}\rangle \simeq 10^{-7}$ for a hard-sphere fluid at is freezing point. All the same a considerable improvement of the statistics on $\langle P_{\text{Acc}}\rangle$ at high densities (in the nematic phase) can be achieved by using a kind of biased sampling to be described below.

In the nematic phase the distribution of molecular orientations is no longer isotropic. Let us denote this distribution by $f(\cos\theta)$ where θ denotes the angle with the nematic director and

$$\int_0^1 f(\cos\theta)\, d\cos\theta = 1, \tag{7}$$

where we have used the fact that $\cos\theta$ is equivalent to $-\cos\theta$. In the dense nematic phase $f(\cos\theta)$ is strongly peaked around $|\cos\theta| = 1$.

It is intuitively clear that the probability of accepting an additional particle is greater if this particle is aligned with the director ($|\cos\theta| \approx 1$) than when the orientation of the particle makes an appreciable angle with the director. This statement can be made more quantitative. Consider all molecules with a given orientation $\cos\theta$ with respect to the director. The density of such molecules is $(N/V)f(\cos\theta)$. Let us consider all molecules with orientation $\cos\theta$ as a distinct chemical species. The chemical potential of this species is given by :

$$\mu = kT \ln\left(\frac{N}{V} f(\cos\theta)\right) + \mu_{\text{EXCESS}}(\cos\theta), \tag{8}$$

where the first term on the right-hand side is the ideal gas chemical potential corresponding to a density $(N/V)f(\cos\theta)$. Of course the total chemical potential of all different ' species ' must be the same. Hence it follows that :

$$kT \ln f(\cos\theta) + \mu_{\text{EXCESS}}(\cos\theta) = \text{constant}. \tag{9}$$

Inserting Widom's expression in (9) we obtain :

$$\left.\begin{aligned} \ln\left(f(\cos\theta)/\langle P_{\text{Acc}}(\cos\theta)\rangle\right) &= \text{constant}, \\ \text{or} \qquad f(\cos\theta) &= c\langle P_{\text{Acc}}(\cos\theta)\rangle \end{aligned}\right\} \tag{10}$$

where $\langle P_{\text{Acc}}(\cos\theta)\rangle$ stands for the probability of accepting an additional particle with orientation $\cos\theta$ with respect to the director. The point to note is that if $\langle P_{\text{Acc}}(\cos\theta)\rangle$ is known at one angle (preferably around $|\cos\theta| \sim 1$) where it is largest) and $f(\cos\theta)$ is known for the same angle (this involves accumulating a histogram of $f(\cos\theta)$ during the Monte Carlo run) then a much better estimate of μ can be obtained from

$$\mu = kT \ln\rho + kT \ln f(\cos\theta = 1) - kT \ln\langle P_{\text{Acc}}(\cos\theta) = 1)\rangle \tag{11}$$

than from the ' brute force ' expression, (6). Typically the acceptance for $|\cos\theta| = 1$ may be a factor 20 higher than the average acceptance for particles thrown in with random orientations.

2.4. *Pressure evaluation at constant volume*

In some cases it is advantageous to perform runs at constant volume rather than at constant pressure. This is true in particular in the vicinity of the phase transition where small fluctuations in the volume, such as normally occur in constant pressure simulations, have a pronounced effect on the nematic order parameter. In order to obtain information about the pressure in constant-volume runs one could in principle make use of the virial expression for the pressure. In practice, use of the virial equation of state requires knowledge of the value of the pair distribution of non-spherical particles at contact, which is a rather complex object. We employed a method to determine the pressure in a constant volume run, which is basically a simple method to determine the relevant part of the pair distribution at contact. As the relation with the virial method is not directly obvious we explain the method used in some detail. The central step in this procedure is to determine whether an attempted Monte Carlo move to decrease the system volume (or, more precisely, to increase the size of the particles) *would* be accepted although, just as in Widom's particle insertion method, no such move is ever carried out. We now proceed to give a more precise description of the procedure referred to in the above sentence. Let us first consider the configurational part of the partition function

$$Q=\frac{1}{N!}\int_v - \int \exp\left(-\beta U(q^N)\right) dq^N$$

$$=\frac{V^N}{V!}\int_0^1 - \int_0^1 \exp\left(-\beta U(\xi^N)\right) d\xi^N. \tag{12}$$

In the second line of (12) we have changed to scaled centre of mass coordinates $\xi_i=(q_i/L)$. In order not to obscure the present derivation with irrelevant detail we omit all reference to internal or orientational coordinates which remain unaffected by the scaling of the centre of mass coordinates.

The contribution to the free energy due to the configurational part of the partition function equals

$$F=-kT\ln Q=-kT\ln\left(V^N/N!\right)-kT\ln q_N(\sigma^3/V) \tag{13}$$

where q_N is defined as :

$$q_N(\sigma^3/V)=\int_0^1 \cdots \int_0^1 \exp\left(-\beta U(\xi^N)\right) d\xi^N. \tag{14}$$

As indicated above q_N is a function of the ratio of the particle size to the system size, σ^3/V.

The contribution to the free energy due to q_N is :

$$F'=F+kT\ln\left(\frac{V^N}{N!}\right)=-kT\ln q_N(\sigma^3/V). \tag{15}$$

As F' is a function of σ^3/V only, it is easy to show that

$$\left(\frac{\partial F'}{\partial V}\right)_\sigma=-\left(\frac{\sigma^3}{V}\right)\left(\frac{\partial F'}{\partial \sigma^3}\right)_V=-\left(\frac{\sigma^3}{V^2}\right)\frac{dF'}{d(\sigma^3/V)}. \tag{16}$$

Now $dF'/d(\sigma^3/V)$ can in principle be obtained from the acceptance of Monte Carlo moves in which one attempts to increase the density $\rho=(N/V)\sigma^3$:

$$\left(\frac{dF'}{d\sigma^3/V}\right)=-NkT\lim_{\Delta\rho\to 0+}\frac{\ln\langle P_{\mathrm{Acc}}\rangle}{\Delta\rho}. \tag{17}$$

The reader can easily verify that, for hard-core systems, it would be incorrect to use the limit $\Delta\rho\to 0-$ in (17). Combining (15), (16) and (17) we get :

$$\left(\frac{\partial F'}{\partial V}\right)_{\sigma}=\left(\frac{\partial F}{\partial V}\right)+\frac{NkT}{V}=-P+\frac{NkT}{V}$$

$$=\frac{\sigma^3}{V^2}\cdot NkT\lim_{\Delta\rho\to 0+}\frac{\ln\langle P_{\mathrm{Acc}}\rangle}{\Delta\rho} \tag{18}$$

and hence :

$$P=\frac{NkT}{V}-\frac{\rho kT}{V}\lim_{\Delta\rho\to+0}\frac{\ln\langle P_{\mathrm{Acc}}\rangle}{\Delta\rho} \tag{19}$$

which relates P to the limiting slope of the logarithm of attempted density increases in the scaled system. Actually we do not compute $\ln\langle P_{\mathrm{Acc}}\rangle/\Delta\rho$ directly. Rather, we reduce $\langle P_{\mathrm{Acc}}\rangle$ to an average property of particle pairs, which is easier to compute. We start with the observation that the probability of acceptance of a volume change is given by the product of the probabilities that none of the $N(N-1)/2$ particle pairs overlap after the density increase :

$$\langle P_{\mathrm{Acc}}\rangle=\left\langle\prod_{i<j}(1-P_{ij}^{\mathrm{overlap}})\right\rangle. \tag{20}$$

In the limit of small $\Delta\rho$ all overlap probabilities $P_{ij}^{\mathrm{overlap}}\ll 1$ and we may expand the product to linear order in P_{ij}.

Defining $\langle P_i^{\mathrm{overlap}}\rangle=\sum_{j\neq i}\langle P_{ij}^{\mathrm{overlap}}\rangle$ we then obtain

$$\langle P_{\mathrm{Acc}}\rangle\approx 1-\frac{N}{2}\langle P_i^{\mathrm{overlap}}\rangle\approx P_0^{N/2}(\Delta\rho) \tag{21}$$

where P_0 is the probability that particle i will not overlap with any of its neighbours after a small density increase $\Delta\rho$. As P_0 is the same for all particles i we have dropped the subscript i. We now introduce a quantity $P_1(\Delta\rho)$ which denotes the probability density that a given particle will experience the first overlap with any of its neighbours if the density is increased by $\Delta\rho$, *irrespective* of whether any other pair of particles has already reached overlap :

$$P_1(\Delta\rho)=-\frac{\partial P_0(\Delta\rho)}{\partial\Delta\rho}. \tag{22}$$

$P_1(\Delta\rho)$ can easily be determined during a Monte Carlo run ; one just has to compute for all particles i what minimum density change is needed to make it overlap with any of its neighbours. A histogram of the resulting distribution is then stored for later analysis. For small values of $\Delta\rho$ $P_1(\Delta\rho)$ is of the form :

$$P_1(\Delta\rho)=\alpha\exp(-\alpha\Delta\rho) \tag{23}$$

corresponding to

$$P_0(\Delta\rho)=\exp(-\alpha\Delta\rho). \tag{24}$$

The constant α is easily determined from a linear, least-squares fit of $\ln P_1(\Delta\rho)$ to $\Delta\rho$.

Knowing α one immediately obtains for $\langle P_{\mathrm{Acc}}\rangle$ (21)

$$\langle P_{\mathrm{Acc}}\rangle = \exp\left(-\frac{N}{2}\alpha V\rho\right) \tag{25}$$

and hence (19):

$$P = \frac{NkT}{V}\left(1+\frac{\rho\alpha}{2}\right), \tag{26}$$

which is our final result. Note that α in (26) depends on the density ρ; as $\rho\to 0$, $\alpha/2$ approaches B_2. As an example we show how this expression trivially yields the virial equation of state for hard spheres.

The average number of spheres in a shell of thickness $d\sigma$ around a given sphere is given by:

$$dn = 4\pi\sigma^2 g(\sigma)\left(\frac{N}{V}\right)d\sigma. \tag{27}$$

We want to compute the average number of spheres that would overlap with a given sphere if the density is increased by an amount $\Delta\rho$ due to a change $d\sigma$ in σ at constant V:

$$\begin{aligned}\Delta n &= \frac{dn}{d\rho}\Delta\rho = \frac{dn}{d\sigma}\frac{d\sigma}{d\rho}\Delta\rho \\ &= 4\pi\sigma^2 g(\sigma)\left(\frac{N}{V}\right)\frac{d\sigma}{d(N\sigma^3/V)}\Delta\rho \\ &= 4\pi\sigma^2 g(\sigma)\Delta\rho/3\sigma^2 = \frac{4\pi}{3}g(\sigma)\Delta\rho.\end{aligned} \tag{28}$$

Hence it follows that in this case $\alpha = (4\pi/3)g(\sigma)$ and therefore

$$P = \frac{NkT}{V}\left(1+\frac{2\pi}{3}\rho g(\sigma)\right) = \frac{NkT}{V}\left(1+\frac{2\pi}{3}\left(\frac{N}{V}\right)\sigma^3 g(\sigma)\right) \tag{29}$$

which is the well-known, hard-sphere virial equation of state. We have tested the above method on systems of hard platelets by comparing constant-volume and constant-pressure runs. We found that the two methods always gave consistent results.

As an example of this consistency we computed a point in the equation of state of 108 hard spheres with both methods. Alder, Hoover and Young [15] found that the pressure P of this system at $\rho = 1{\cdot}2298$ equals $P = 27{\cdot}829 \pm 0{\cdot}002$. We find at constant $P = 27{\cdot}829$ an average density $\rho = 1{\cdot}229 \pm 0{\cdot}003$. At a constant density $\rho = 1{\cdot}2298$ we find $P = 27{\cdot}63 \pm 0{\cdot}10$. Both results are mutually consistent, and consistent with the results of [15]. Further evidence for the equivalence of constant-P and constant-V MC is to be found in table 1.

2.5. *Nematic order parameter*

The essential difference between a nematic and an isotropic fluid is that the distribution of molecular orientations has cylindrical symmetry in the nematic

Table 1. Summary of results of Monte Carlo simulations on infinitely thin, hard platelets. Constant pressure runs are indicated by a '*P*' in column 6, constant volume runs by a '*V*'. The order parameter *S* is the average of the largest eigenvalue of the tensor order parameter **Q** (see below (34)). The length of the run in 'sweeps' (=moves/particle) is shown in the last column.

P	ρ	μ	S	N	Ensemble		Sweeps/10^3
1	0·678	0·538		100	*P*		4
1·78	1	1·487	0·09	100		*V*	40
2	1·075	1·697		100	*P*		4
3	1·41			100	*P*		4
3·27	1·5	2·79	0·10	100		*V*	40
4	1·65			100	*P*		4
5	1·88	3·85		100	*P*		40
5·57	2	4·01	0·11	100		*V*	40
7	2·30	4·64		100	*P*		4
9	2·69	5·68		100	*P*		40
9·80	2·82	5·82	0·16	100		*V*	40
11	3·09	6·25		100	*P*		40
11·6	3·16	6·38	0·16	100		*V*	40
12	3·21	6·39		100	*P*		40
13	3·49	6·80		100	*P*		40
13·1	3·49	6·86	0·11	800		*V*	160
14	3·67	7·05		400	*P*		80
14·2	3·75	7·14	0·11	800		*V*	160
14·5	3·87			400	*P*		160
14·8	4·00	7·32	0·36	800		*V*	160
15·0	4·27	7·37		400	*P*		80
15·1	4·24	7·33	0·52	800		*V*	160
15·4	4·49	7·47	0·61	800		*V*	160
15·5	4·61			400	*P*		80
16·0	4·71	7·62		400	*P*		80
16·0	4·90	7·62		100	*P*		80
16·9	5·28	7·76	0·82	100		*V*	40
17·0	5·39	7·83		100	*P*		40
18·0	5·81	8·00		100	*P*		40
18·5	5·98	8·09	0·87	100		*V*	40
19·1	6·18	8·17	0·88	100		*V*	40
19·8	6·45	8·27	0·89	100		*V*	40
20·0	6·35			100	*P*		40
21·0	6·79	8·44	0·90	100		*V*	40
22·0	7·17	8·56		100	*P*		40
23·4	7·68	8·80	0·93	100		*V*	40
24·0	7·94	8·86		100	*P*		40

phase instead of the spherical symmetry that is found in isotropic fluids. A set of order parameters quantify the non-sphericity of the orientational distribution function $f(\theta, \phi)$ [16]. For an axially symmetric distribution the most general form of $f(\theta, \phi)$ is independent of ϕ :

$$f(\theta) = \sum_{l=0}^{\infty} a_{2l} P_{2l}(\cos\theta) \tag{30}$$

where θ is the angle of the molecular orientation with the axis of symmetry (the nematic director). For an isotropic fluid all a_{2l} with $l>0$ vanish. The coefficients a_{2l} are related to the average values of $\langle P_{2l}(\cos\theta)\rangle$ in the nematic phase :

$$\langle P_{2l}(\cos\theta)\rangle = \left(\frac{2}{4l+1}\right) a_{2l}. \tag{31}$$

The quantities $\langle P_{2l}(\cos\theta)\rangle$ play the role of order parameters. Usually the lowest non-trivial order parameter, i.e. $\langle P_2(\cos\theta)\rangle$ is referred to as *the* nematic order parameter. In a computer simulation this order parameter could in principle be evaluated using :

$$S = \frac{1}{N}\left\langle \sum_{i=1}^{N} \left(\tfrac{3}{2}\cos^2\theta_i - \tfrac{1}{2}\right)\right\rangle \tag{32}$$

where θ_i is the angle of the ith molecular axis with the nematic director. In practice, however, the orientation of the nematic director is now known *a priori*. Hence what one can actually compute is

$$\begin{aligned} S' &= \frac{1}{N}\left\langle \sum_{i=1}^{N} \left(\tfrac{3}{2}(\mathbf{n}\cdot\mathbf{u}_i)^2 - \tfrac{1}{2}\right)\right\rangle \\ &= \frac{1}{N}\sum_{i=1}^{N} \langle \mathbf{n}\cdot\left(\tfrac{3}{2}\mathbf{u}_i\mathbf{u}_i - \tfrac{1}{2}\mathbf{I}\right)\cdot\mathbf{n}\rangle \\ &= \frac{1}{N}\sum_{i=1}^{N} \langle \mathbf{n}\cdot\mathbf{Q}\cdot\mathbf{n}\rangle, \end{aligned} \tag{33}$$

with

$$\mathbf{Q}_i \equiv \tfrac{3}{2}\mathbf{u}_i\mathbf{u}_i - \tfrac{1}{2}\mathbf{I}$$

for an arbitrary unit vector $\mathbf{n}$.

The tensor order parameter $\langle\mathbf{Q}\rangle$ defined by :

$$\langle\mathbf{Q}\rangle = \frac{1}{N}\sum_{i=1}^{N} \langle\mathbf{Q}_i\rangle \tag{34}$$

is a traceless symmetric 2nd-rank tensor, with three eigenvalues λ_+, λ_0, λ_-. We can define the nematic order parameter S as the largest positive eigenvalue (λ_+) of $\langle\mathbf{Q}\rangle$. The nematic director is given by the corresponding eigenvector. The same procedure has been followed before by several other authors [17, 18]. Note that the present definition of the order parameter forces the order parameter to be positive. In the nematic phases this presents no special problems. However, such a procedure will also lead to small ($O(N^{-1/2})$) positive values of the order parameter in the isotropic phase. For some applications it is

preferable to use a different definition of the order parameter, namely $S = -2\lambda_0$, where λ_0 is the middle eigenvalue of $\langle \mathbf{Q} \rangle$. In the nematic phase $\lambda_0 \approx \lambda_- = -\frac{1}{2}\lambda_+$ and the present definition coincides with the previous one. In the isotropic phase the present definition yields an order parameter which fluctuates around an average that is much closer to zero ($O(1/N)$); typically $|\langle \lambda_0 \rangle| < 0{\cdot}01$. This definition of the order parameter was employed in our investigation of the validity of the Landau–de Gennes description of order parameter fluctuations in the isotropic phase (see § 3.3). The system size dependence of the different eigenvalues of $\langle \mathbf{Q} \rangle$ is discussed in more detail in the Appendix.

3. Results and discussion

3.1. *Overview*

In this section we present the result of constant-P and constant-V Monte Carlo simulations on a system of N hard platelets with $N = 25$, 50, 100, 400 and 800. Most runs were carried out for the 100 particle system. A typical run involved 4×10^4 moves/particle (i.e. 4×10^6 moves for the $N = 100$ system). Some runs close to the phase transition were 2–4 times longer. Every run was preceded by an equilibration run of several thousand sweeps (= moves/particle). In general a new run started from the equilibrated configuration at a slightly higher or lower pressure. The phase diagram was traversed in the direction of both increasing and decreasing pressure to test for hysteresis effects. A typical run took 1–2 hours of CPU time on a CDC CYBER 175/100.

The discussion of the results of the Monte Carlo simulations is organized as follows : in § 3.2 we present the data on the equation of state of hard platelets in the isotropic phase and we compare the results with (*a*) a five-term virial equation of state (*b*) the Onsager expression and (*c*) a scaled-particle prediction. In the same section we discuss the determination of the isotropic–nematic phase transition and compare our findings with the relevant theoretical predictions. We conclude § 3.2 with a discussion of the limiting form of the high-density equation of state.

Section 3.3 deals with the density dependence of the nematic order parameter. We also analyse order parameter fluctuations in the isotropic phase, their statistical nature and spatial correlations. These results are discussed in the light of the Landau–de Gennes and Maier–Saupe theories.

3.2. *Phase diagram*

Figure 3 shows the equation of state of the hard-platelet fluid as obtained by constant-pressure and constant-volume Monte Carlo simulation. Most points were obtained for a 100 particle system. However, we looked for possible N-dependences of the results by running both larger and smaller systems. Only around the I–N phase transition was there any evidence for a systematic system size dependence of the equation of state. This system size dependence became smaller than our computational accuracy for system-sizes with $N \geqslant 400$. For this reason, the points in the region round the I–N transition ($3{\cdot}5 < \rho^* < 4{\cdot}5$) refer to simulations on systems of 400 or 800 particles. A summary of all runs is given in table 1. Notice that figure 3 combines the information on the pressure dependence of the density ρ and the pressure dependence of the chemical potential as determined by Widom's particle insertion method. In order to test

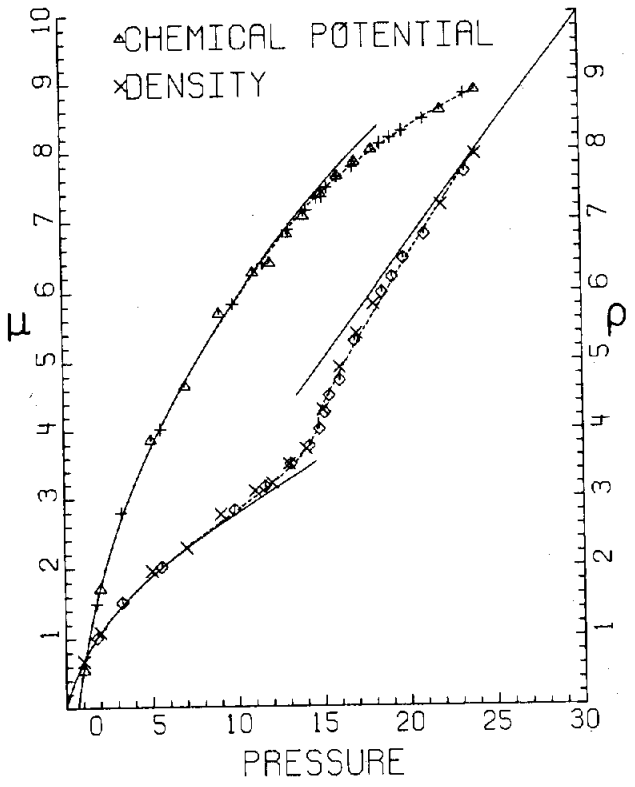

Figure 3. Equation of state of infinitely thin hard platelet fluid. The left-hand ordinate refers to the chemical potential (+ and △), the right-hand ordinate denotes the density (× and ◇). Both constant-pressure (△ and ×) and contant-volume (+ and ◇) data are shown. For the sake of legibility only a fraction of all MC results are represented. At high pressures pressure dependence of the density approaches the relation $\rho = P/3$ (44) which is shown as a straight drawn line. At pressures below $P \approx 10$ both ρ and μ are very close to the 5-term virial expressions (drawn curves). The dashed curves have been drawn to guide the eye.

the quality of the low density MC results we also computed the first 5 virial coefficients of the hard-platelet fluid. In fact, the 2nd virial coefficient is known exactly (1), $B_2/\sigma^3 = \pi^2/16$. We evaluated virial coefficients 3–5 by Monte Carlo using the diagram technique developed by Ree and Hoover [19]. The values of B_2 through B_5 are summarized in table 2. Note that while B_3 is fairly large, B_4 is quite small and B_5 is small but negative. Although it is well known that virial coefficient higher than the 3rd can in principle be negative for repulsive, hard-core systems we are not aware of any previous example where a virial coefficient as low as B_5 was in fact found to be negative for a dimensionality as low as 3 (or actually 2, as we find the same for hard needles in 2D [20]).

Comparing the virial equation of state with the Monte Carlo data (see figure 3) we find excellent agreement up to a reduced density $\rho \approx 2$. We also find good agreement between the 5-term virial expression for the chemical potential

$$\mu/kT = \ln \rho + \sum_{n=2}^{5} (n/n-1) B_n \rho^{n-1}, \tag{35}$$

and the MC results.

Table 2. Virial coefficients of infinitely thin hard platelets of diameter σ. B_3 through B_5 were obtained numerically. Note that $B_5 < 0$.

n	B_n/σ^3	$B_n/B_2{}^{n-1}$
2	$\pi^2/16$	1
3	$0{\cdot}1692 \pm 0{\cdot}0001$	$0{\cdot}4447 \pm 0{\cdot}0003$
4	$0{\cdot}00480 \pm 0{\cdot}00009$	$0{\cdot}0205 \pm 0{\cdot}0005$
5	$-0{\cdot}00867 \pm 0{\cdot}00016$	$-0{\cdot}0599 \pm 0{\cdot}0011$

Note also that at reduced pressures above $P\sigma^3/kT \approx 10$ the virial equation of state predicts a lower density than we find in the MC simulations. This suggests that at least one of the higher virial coefficients B_n $(n \geqslant 6)$ must also be negative.

Let us next compare the MC equation of state with two theoretical predictions viz, the Onsager theory [2] and a version of the scaled particle theory [21]. Comparing the results of the Onsager theory, which was designed to describe the equation of state of thin hard rods, with data found for a system of infinitely thin hard platelets may at first sight appear to be not very illuminating, but actually such a comparison is quite interesting for the following reason: the excluded volume of two long cylindrical rods of length L and diameter D $(L \gg D)$ is of the form:

$$v_{12}{}^{R}(\theta) = 2L^2 D|\sin\theta| + \mathcal{O}(D/L), \tag{36}$$

where θ is the angle between the molecular axes of the rods. If we compare this expression with the excluded volume of a pair of infinitely thin platelets of diameter σ:

$$v_{12}{}^{P}(\theta) = \frac{\pi\sigma^3}{2}|\sin\theta| \tag{37}$$

it is clear that at the level of pair excluded volumes (i.e. to 'second virial' level) the platelet system and the thin rod $(L/D \to \infty)$ system are equivalent [1]. The Onsager equation of state becomes exact in the limit $L/D \to \infty$, because in that limit all higher virial coefficient of the hard rod fluid vanishes. However, the Onsager equation of state is not an exact description of the hard-platelet fluid because in this case the higher virial coefficients do not vanish (see table 2). What makes the comparison of the hard-platelet MC results with the Onsager theory interesting is that any discrepancy between the two is exclusively due to the effect of the higher virial coefficients. It turns out that the Onsager approximation $(P/kT = \rho + B_2\rho^2)$ to the hard-platelet equation of state yields pressures that are consistently too low in the isotropic region (see figure 4). However, the deviations are never very large due to the strong degree of cancellation of higher virial terms. In fact an equation of state which includes both the exact B_2 and B_3 would do much worse than the Onsager theory. Still, the Onsager theory yields a very poor estimate of the I–N phase transition as will be discussed below. We have also compared our low-density equation of state data with theoretical predictions based on a version of the scaled particle theory for hard cylinders [81]. If we take the limit of infinitely thin platelets in the expression given by Savithramma and Madhusudana, we obtain an equation of state for the isotropic phase which is of the form:

$$P/kT = \rho + B_2\rho^2 + B'_3\,\rho^3, \tag{38}$$

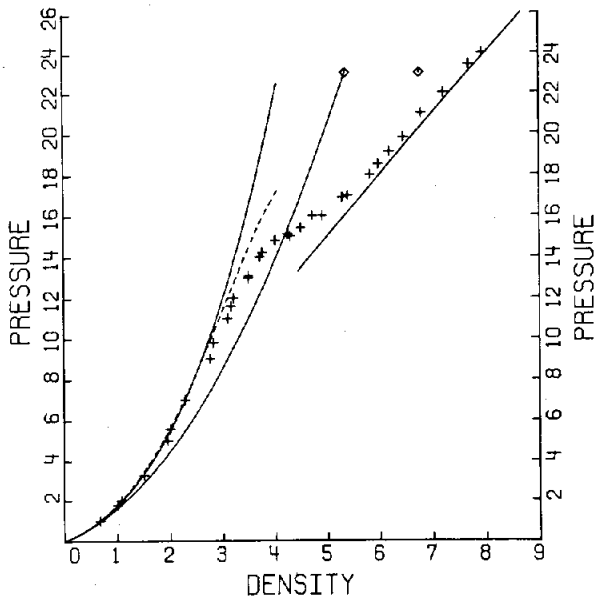

Figure 4. Hard platelet equation of state (+) compared with: (1) Onsager expression (lower drawn curve); (2) scaled particle theory of [19] (upper drawn curve); (3) 5-term virial series (dashed curve); (4) $P=3\rho$ (44) (drawn straight line). The end of the isotropic branch and the beginning of the nematic branch as predicted by the Onsager theory are indicated by: ◇

where B_2 is the exact second virial coefficient but B'_3 is not equal to the real third virial coefficient. In fact, $B'_3/B_2^2=0{\cdot}333$ rather than $0{\cdot}445$. The resulting equation of state is reasonably good at low densities but tends to overestimate the pressure at high densities (see figure 4). For example, at the density where we observe the I–N transition the scaled particle pressure is off by some 50 per cent (in contrast, the Onsager equation, somewhat fortuitously, is off by only a few per cent at the same density). This result indicates that scaled particle theory, at least the version used in [21], does not lead to an improved description of the isotropic phase.

We now come to the location of the isotropic–nematic transition. Before discussing the Monte Carlo data on the I–N transition we should mention a few computational aspects. First of all, fluctuations in the system become very sluggish in the vicinity of $\rho\approx 4$ and rather long runs (typically $1{\cdot}6\times 10^5$ moves/particle) were needed to obtain good statistics. Moreover, a considerably longer time was spent on equilibration (typically $2{\cdot}5\times 10^4$ moves/particle, instead of 5×10^3). In this region we also found evidence for a pronounced system size dependence of the MC results, as can be seen from table 3. No such system size dependence was observed at either higher or lower densities. Finally we should mention that we never found any evidence for hysteresis. This is somewhat surprising as the I–N transition in 3D is supposed to be first order. One should bear in mind however that real thermotropic liquid crystals cannot be superheated at the I–N transition. To locate the isotropic–nematic phase transition we proceeded as follows: the condition for two phases to be in thermodynamic equilibrium is

Table 3. System size dependence of density ρ at constant pressure close to the I–N phase transition. Left: $P=14$, Right: $P=15$.

N	$\rho(P=14)$	$\rho(P=15)$
50	3·94	4·65
100	3·72	4·33
400	3·67	4·27
800	3·68	4·26

that the pressure and the chemical potential of both phases to be equal. As we determine both μ and P by Monte Carlo it is in principle straightforward to find the phase transition. However, as the phase transition that we find shows no hysteresis we cannot locate the transitions by searching for the point where the chemical potential branches corresponding to the two phases intersect. We therefore follow a slightly different approach. We make use of the thermodynamic relation $(\partial\mu/\partial P)_{T,N}=\rho^{-1}$. Hence μ at high pressures can be computed by integration:

$$\mu(P_2)=\mu(P_1)+\int_{P_1}^{P_2}\rho^{-1}(P)\,dP. \tag{39}$$

At sufficiently low densities, where the virial equation of state is reliable, we know μ exactly. We can now compute μ at high pressures (in the nematic phase) by integrating:

$$\mu(P_{\mathrm{HIGH}})=\mu(P_{\mathrm{LOW}})+\int_{P_{\mathrm{LOW}}}^{P_{\mathrm{IN}}}\rho_{\mathrm{I}}^{-1}(P)\,dP+\int_{P_{\mathrm{IN}}}^{P_{\mathrm{HIGH}}}\rho_{\mathrm{N}}^{-1}(P)\,dP, \tag{40}$$

where P_{IN} is the, as yet unknown, pressure of the I–N transition. ρ_{I} and ρ_{N} are polynomical fits to the density as a function of pressure in the isotropic and nematic phases. Clearly, the value of $\mu(P_{\mathrm{HIGH}})$ thus obtained depends on the choice of P_{IN}. We fix our choice of P_{IN} by by requiring that the $\mu(P_{\mathrm{HIGH}})$ computed from (40) matches the chemical potential at the same pressure as obtained from Widom's particle insertion method. In this way we locate the I–N phase transition at a pressure $P=14{\cdot}8$ with the densities of the co-existing isotropic and nematic phases given by $\rho_{\mathrm{I}}=4{\cdot}04$ and $\rho_{\mathrm{N}}=4{\cdot}12$. Even with this method the density gap at the I–N transition cannot be determined very accurately and it may in fact be even smaller than quoted here. Note that our present results for the pressure of the I–N transition differ by a few per cent from the value we gave in a preliminary publication [22]. If we now compare the present results with the predictions for the I–N transition based on a numerical solution of the Onsager model [23, 24] we observe a very large discrepancy. The Onsager theory predicts a very strong first order phase transition at $P=23{\cdot}01$ (cf. $P^{\mathrm{MC}}=14{\cdot}8$) with $\rho_{\mathrm{I}}=5{\cdot}35$ and $\rho_{\mathrm{N}}=6{\cdot}75$ (cf. $\rho_{\mathrm{I}}{}^{\mathrm{MC}}=4{\cdot}04$, $\rho_{\mathrm{N}}{}^{\mathrm{MC}}=4{\cdot}12$). Hence instead of a density jump of less than 2 per cent as found in the present simulation, the Onsager theory predicts a value of $\Delta\rho/\rho\approx 26$ per cent! As mentioned before, any discrepancy between the Onsager theory and the present results is exclusively due to the neglect of higher order virial terms in this theory. Clearly, for hard platelets this approximation is not warranted. We should hasten to add that Onsager

never suggested that the theoretical results he had obtained should be applicable to anything but thin rods. We just wish to stress that for the present very simple model system none of the current statistical mechanical theories of the I–N transition that we are aware of seem to work.

We conclude this section with a discussion of the equation of state in the dense nematic. At high pressure the equation of state of the dense nematic rapidly approaches the limiting form $P=3\rho$ (see figure 3). Incidentally, this result also follows from the Onsager theory [2]. Below we show that this result is actually quite model independent, it can be derived by a simple scaling argument. Consider the free energy of a hard-core nematic, which is of the form :

$$F/kT=\ln\rho+\int_{-1}^{1} f(\cos\theta)\ln f(\cos\theta)\,d\cos\theta+(\text{excluded volume terms}). \quad (41)$$

At high densities the orientation of platelets is restricted by the presence of other similarly aligned platelets. The width of the distribution function $f(\cos\theta)$ can be estimated by noting that on the average each particle can move in a cylindrical box of diameter σ and height a, such that $V_0=\pi\sigma^2 a=1/\rho$. The width of the orientational distribution function is then limited by the angle over which a platelet can rotate in its box. This angle, θ_{MAX} is of order $a/\sigma\sim 1/\rho$. Let us assume that $f(\cos\theta)$ is approximately constant in the interval $\cos\theta_{\mathrm{MAX}}\leqslant|\cos\theta|\leqslant 1$. As $f(\cos\theta)$ must be normalized to 1, it then follows that $f(\cos\theta)\approx 1/\theta^2{}_{\mathrm{MAX}}$ for $\cos\theta_{\mathrm{MAX}}\leqslant|\cos\theta|\leqslant 1$. Hence :

$$F/kT\approx\ln\rho+\ln\theta_{\mathrm{MAX}}{}^{-2}+(\text{excluded volume terms}). \quad (42)$$

But as θ_{MAX} is $1/\rho$ it follows that

$$F/kT\approx 3\ln\rho+(\text{excluded volume terms}). \quad (43)$$

From which it follows that

$$P=3\rho+(\text{excluded volume terms}). \quad (44)$$

Of course it remains to be shown that the remaining terms are small. This is indeed the case, as the leading contribution to the free energy due to the excluded volume terms is a constant which does not contribute to the pressure ; all higher order terms are $\mathcal{O}(1/\rho)$. Incidentally, we note that a similar relation holds for hard needles in 2D, viz. $P=2\rho$ as $\rho\to\infty$ (20). As can be seen from figure 3 the relation $P=3\rho$ is satisfied to better than 2 per cent for $\rho>5{\cdot}5$.

We should add that the fact that the free energy of the hard platelet system increases only slowly with density severely limits its potential use as a hardcore reference system for thermodynamic perturbation theories (see, e.g. [6] and references therein). This is so because the contribution of long range attractive forces to the free energy will go as $-a\rho$. At sufficiently high densities this term will overwhelm the repulsive $\ln\rho$ term and the system will collapse. Of course this problem is peculiar to systems with zero volume.

3.3. *Nematic order parameter*

The density dependence of the nematic order parameter was determined using the largest eigenvalue method mentioned in § 2.5. The Q tensor was diagonalized for every individual configuration and the resulting eigenvalues were averaged.

It has been suggested [17] that it might be useful to average the Q-tensor over a number of MC configurations before diagonalizing. We feel however that this is a risky procedure because subchain averages in a MC run have no statistical mechanical meaning in situations where the average tends to zero as the subchain becomes infinitely long. In contrast, our definition of the order parameter yields a quantity that is a well behaved canonical average. In figure 5 the density dependence of the order parameter $\langle P_2 \rangle \equiv S$ is shown for systems of 100, 400 and 800 platelets. The data shown in this figure have been collected in table 5. In the dense nematic phase we observed little N-dependence of the

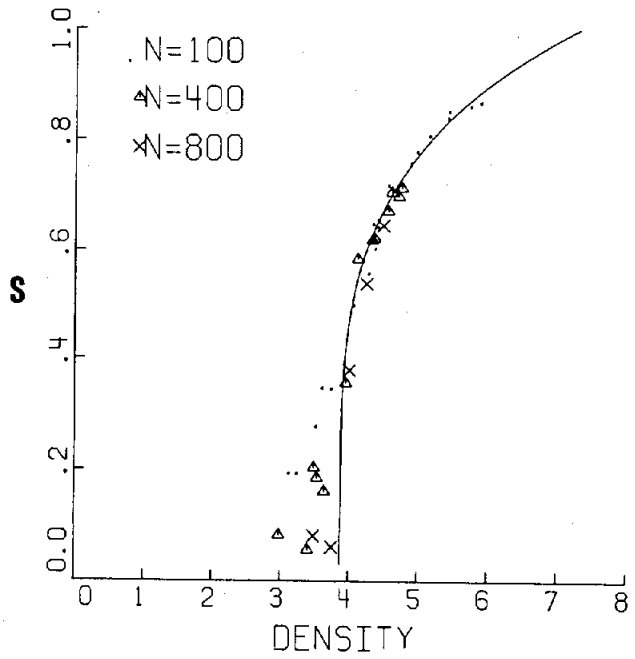

Figure 5. Density dependence of the nematic order parameter of a hard platelet fluid. Close to the I–N transition a pronounced system size dependence is observed (●, $N=100$; △, $N=400$; ×, $N=800$). The order parameter was computed from the largest eigenvalue on the tensor order parameter **Q** (see below (34)). The drawn curve is a fit to a relation of the form $S=c(\rho-\rho_c)^\beta$ with $\beta=0{\cdot}25$.

Table 4. Comparison of $\langle P_2(\cos\theta(r))\rangle$ at $r=L/2$ ($L=$boxlength) and S^2. Note that even for the rather small system sizes considered ($N=100$), there is good agreement between the two estimates of S^2.

$P_2(L/2)$	S^2	ρ^*
0·017	0·035	3·16
0·215	0·221	3·87
0·425	0·410	4·49
0·656	0·668	5·28
0·863	0·867	8·16

Table 5. Density dependence of the nematic order parameter computed from the *largest* eigenvalue of the Q-tensor for system sizes $N=100$, $N=400$ and $N=800$.

ρ	S		
	$N=100$	$N=400$	$N=800$
2·00	0·121	—	—
2·98	—	0·082	—
3·09	0·192	—	—
3·16	0·187	—	—
3·21	0·192	—	—
3·40	—	0·056	—
3·49	0·276	0·203	0·081
3·53	—	0·185	—
3·58	0·345	—	—
3·64	—	0·160	—
3·71	0·343	—	—
3·75	—	—	0·061
3·87	0·470	—	—
3·95	—	0·354	—
4·00	—	—	0·377
4·03	0·495	—	—
4·12	—	0·582	—
4·25	0·555	—	0·536
4·32	0·646	—	—
4·33	—	0·617	—
4·34	0·600	—	—
4·36	—	0·621	—
4·39	0·641	—	—
4·49	0·640	—	0·645
4·54	0·716	—	—
4·56	—	0·671	—
4·61	—	0·705	—
4·71	—	0·697	—
4·76	—	0·712	—
4·86	0·756	—	—
4·95	0·776	—	—
5·12	0·804	—	—
5·28	0·817	—	—
5·39	0·835	—	—
5·41	0·847	—	—
5·71	0·856	—	—
5·86	0·863	—	—
7·93	0·930	—	—
8·16	0·931	—	—

order parameter, but close to the transition we observe a rather strong N dependence, in particular in the isotropic phase where S should vanish in the thermodynamic limit. We find that below $\rho \approx 4$ the apparent values of the order for the 800 particle system become quite small. We have tried to fit the density dependence of the order parameter to a power law of the form $S = c(\rho - \rho_c)^\beta$. As can be seen from figure 6 we get a very acceptable fit over almost 2 decades in $\epsilon = (\rho - \rho_c)/\rho_c$ with a value $\rho_c = 3{\cdot}8 \pm 0{\cdot}2$ and $\beta = 0{\cdot}23 \pm 0{\cdot}03$. We should add that we were unable to fit the Monte Carlo data to an expression of the above form but with $\beta = \frac{1}{2}$ which is the classical exponent for the density dependence of the order parameter in an (almost) second order phase transition. These Monte Carlo findings are also interesting because a similar behaviour of the order parameter has been observed in real thermotropic liquid crystals [25, 26] and

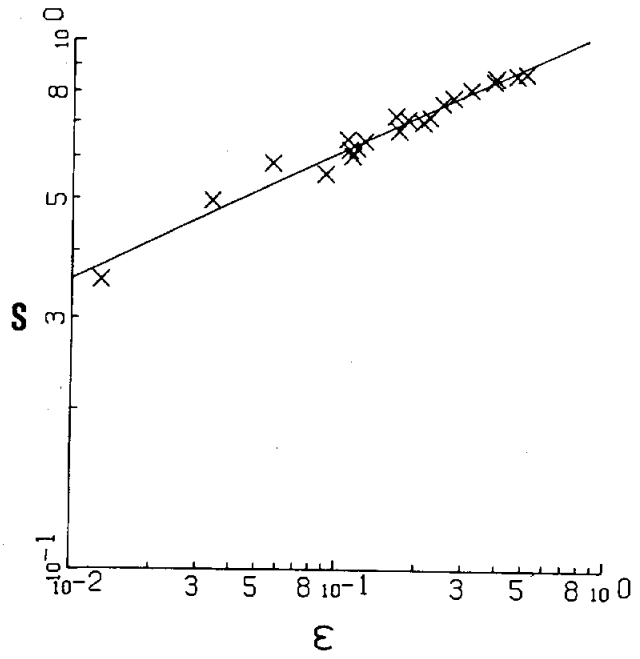

Figure 6. Dependence of log S on log ϵ ($\epsilon \equiv (\rho - \rho_c)/\rho_c$). The straight line corresponds to a fit of the form $S = c(\rho - \rho_c)^\beta$ with $\beta = 0{\cdot}23$. Note that the power law behaviour seems to be satisfied over almost 2 decades of ϵ.

it has been suggested [26] that the observed behaviour is a consequence of the fact that the I–N transition is almost tri-critical, in which case one should expect to find an exponent $\beta = 1/4$. It should be added however, that recent experiments [27] have failed to produce any evidence supporting this conjecture. In order to get a better understanding of the density dependence of the order parameter in the nematic phase we decided to study order parameter fluctuations in the isotropic phase. The reason for doing so is the following : if the Landau theory for (almost) second order phase transitions were applicable it should be possible to expand the free energy of the liquid crystal forming fluid in powers of the order parameter :

$$F(S) = F_0 + AS^2 + BS^3 + CS^4 + \ldots . \tag{45}$$

The usual assumption is then that $A = a(\rho_0 - \rho)$ while B, C, etc., change only slowly in the vicinity of the phase transition. In the special case $B = 0$, the Landau theory would predict a second order I–N phase transition and the density dependence of S in the nematic phase would be given by $S = (a/2C)^{1/2}(\rho - \rho_0)^{1/2}$. In fact, as there is no symmetry reason why B should be zero in the case of nematic liquid crystals, the Landau theory predicts a (weak) first order I–N transition. Of course the crucial assumption in describing phase transitions by a Landau free energy of the form (45) is that the coefficients A, B, C, etc. are slowly varying, well behaved functions of ρ. In a Monte Carlo simulation we can 'measure' the free energy due to order parameter fluctuations directly because the probability of observing a particular value of S is given by [28] :

$$P(S) = c \exp(-\beta F(S)) \tag{46}$$

Hence by collecting a histogram of order parameter fluctuations during an MC run we can obtain information about the coefficients A, B, C, etc., by fitting a polynomical in S to ln $P(S)$. In practice this is a rather tricky operation ; it is quite easy to get good statistics on A, but information about B, C, etc., resides in the wings of the distribution where the statistics are poor. Going to larger systems makes the situation worse because the free energy associated with a given order parameter fluctuation is an extensive variable, hence a linear increase in the system size leads to an exponential decrease in the probability of observing a particular fluctuation. On the other hand going to very small system sizes is not advisable either because for small systems we should expect a pronounced N-dependence of the thermodynamic properties, in particular close to the phase transition. Most of the results we present below were obtained for a 100 particle system ; we studied fluctuations of the middle eigenvalue of the Q-tensor for reasons discussed in the Appendix. Figure 7 shows the density dependence of the coefficient of S^2 in the Landau free energy. We note that this coefficient A,

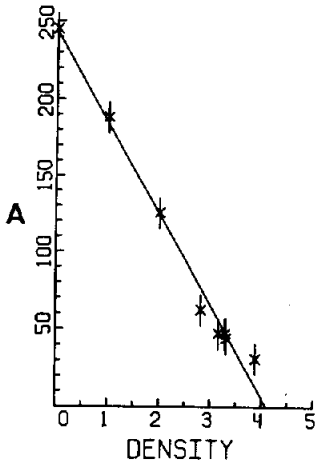

Figure 7. Density dependence of the coefficient of S^2 in the Landau–de Gennes expression for the free energy of the isotropic phase : $F(S) = F_0 + AS^2 + BS^3 + cS^4$. Note that $A \approx a(\rho_c - \rho)$ with $\rho_c = 4{\cdot}10$ (i.e. very close to the I–N transition density).

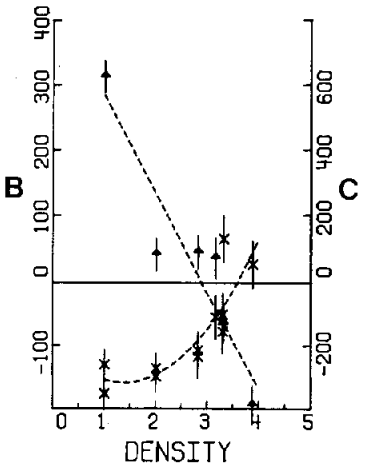

Figure 8. Density dependence of B and C coefficient in de Landau–de Gennes free energy (45), $F(S)=F_0+AS^2+BS^3+cS^4$. ×, B; △, C. Estimated errors in B are indicated by vertical bars. The errors in C cannot easily be estimated, they are probably of the order of 50–100 per cent. The dashed lines serve no other purpose than connecting the data points. Note that at the I–N transition ($\rho\approx4$) B is very close to zero. The data suggest that C may change sign before the I–N transition.

fits very well to a relation of the form $A=a(\rho_0-\rho)$ with $\rho_0\simeq4{\cdot}1$. As expected, A changes sign just at the observed I–N transition. The density dependence of the coefficient of S^3 is shown in figure 8. Note that the estimated error in B is appreciable. Nevertheless it is clear that B is not at all weakly density dependent. In fact, the figure strongly suggest that B goes to (or through) zero somewhere in the vicinity of the I–N transition. The statistics on the coefficients of $S^4(C)$ are so poor that one should consider the data points shown in figure 8 with some scepticism. If one is willing to take these data points seriously they seem to indicate that C too is changing rapidly with density and may even change sign at a density below ρ_{IN}. These results cast severe doubt on the applicability of the normal Landau–de Gennes theory for the description of the isotropic–nematic transition. To return to the question of the possible vicinity of a tricritical point near the I–N transition we note that one way to get a tri-critical point is with a free energy of the form :

$$F(S)=F_0+a(\rho_0-\rho)S^2+CS^4+DS^6+\ldots, \tag{47}$$

with $C>0$, $D>0$. If C for some reason happens to change sign the phase transition changes from second order to first order; the point $C=0$ is a tri-critical point. At that point the density dependence of the order parameter is given by $S=(a/3D)^{1/4}(\rho-\rho_0)^{1/4}$. Clearly, there is no *a priori* reason why the coefficient of S^3, S^4 and S^5 should vanish in the vicinity of the I–N transition. We just wish to point out that the results shown in figure 8 hint at the possibility that the coefficients of S^3 and S^4 may be anomalously small around the I–N transition. Why this should be so is not at all clear.

One quantity that is of interest in any description of the I–N transition is the correlation length of the nematic order parameter. Information about the spatial

extent of orientational correlations is contained in the full, orientation dependent pair distribution function [16, 29] :

$$g(\boldsymbol{\Omega}_1, \mathbf{r}_{12}, \boldsymbol{\Omega}_2) = \sum_{l_1, l_2, l_3} g^{l_1 l_2 l_3}(r) \sum_{m, m', m''} \times \begin{pmatrix} l_1 l_2 l_3 \\ m m' m'' \end{pmatrix} Y_{l_1 m}(\boldsymbol{\Omega}_1) Y_{l_2 m'}(\boldsymbol{\Omega}_{12}) Y_{l_3 m''}(\boldsymbol{\Omega}_2). \quad (48)$$

We have computed the following contributions to this pair distribution function : (1) $g^{000}(r)$, the ' normal ' isotropic radial distribution function, (2) $g^{202}(r)$, which measures the r_{ij} dependence of $\langle P_2(\mathbf{l}_i \cdot \mathbf{l}_j)\rangle$. In the nematic phase $\lim_{r\to\infty} g^{202}(r) = \langle P_2\rangle^2$, (3) $g^{404}(r)$ which is analogous to $g^{202}(r)$ with the difference that it measures correlations of the type $\langle P_4(\mathbf{l}_i \cdot \mathbf{l}_j)\rangle$. In the nematic phase $\lim_{r\to\infty} g^{404}(r) = \langle P_4\rangle^2$.

Figures 9 to 11 show the density dependence of $g^{000}(r)$, $g^{202}(r)$ and $g^{404}(r)$. To be more precise, the latter two figures contain the ratios $g^{202}(r)/g^{000}(r) = \langle P_2(\cos\theta(r))\rangle$ and $g^{404}(r)/g^{000}(r) = \langle P_4(\cos\theta(r))\rangle$. Let us first consider figure 9. Two features will immediately strike the reader who is familiar with radial distribution functions in simple liquids. The first is that $g(r)$ is non-zero for quite short distances in particular at high densities. This is actually not surprising as the centres of parallel platelets can get arbitrarily close. Clearly, the transition to the nematic phase makes it easier for platelets to come close together ; this seems to be reflected in the rather pronounced density dependence of $g(r)$ around $r \approx 0{\cdot}3\sigma$, especially close to the I–N transition. Another, even more striking feature is the almost total absence of structure in $g(r)$ beyond the cusp-like feature at $r \approx \sigma$. The density dependences $g_2(r) = \langle P_2(\cos\theta(r))\rangle$ and $g_4(r) \equiv \langle P_4(\cos\theta(r))\rangle$ resemble one another ; below ρ_{I-N} both decay very rapidly. In the isotropic phase we can define a correlation length ξ_2 (ξ_4) by :

$$\xi_{2l} \equiv \lim_{r\to\infty} \left(-\frac{d}{dr} \ln (g_{2l}(r)) \right)$$

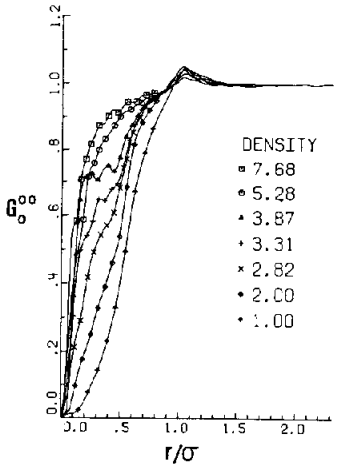

Figure 9. Density dependence of the isotropic part of the radial distribution function, $g^{000}(r)$. Around $r = \sigma$ the distribution function has a cusp-like feature.

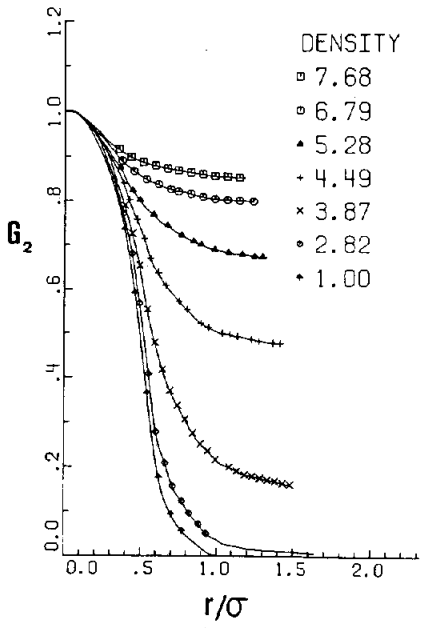

Figure 10. Density dependence of $\langle P_2(\cos(\theta(r)))\rangle \equiv g_2(r)$ (see text below (48)). In the nematic phase $\lim_{r\to\infty} g_2(r) = S^2$ (see table 4).

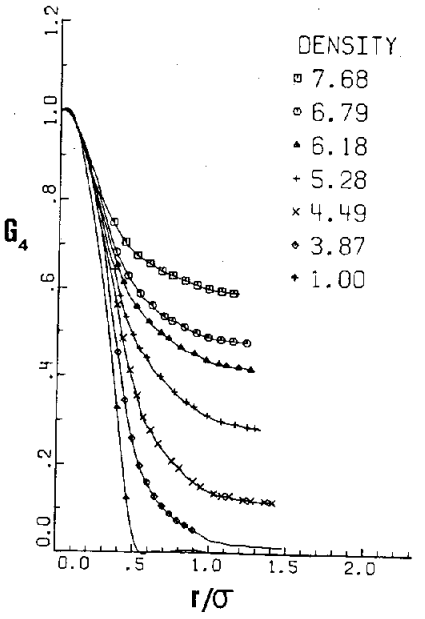

Figure 11. Density dependence of $\langle P_4(\cos(\theta(r)))\rangle \equiv g_4(r)$ (see text below (48)). In the nematic phase $\lim_{r\to\infty} g_4(r) = \langle P_4\rangle^2$.

We find that at densities well below the I–N transition ξ_2 and ξ_4 are small compared to σ. Hence the relevant 'bare' correlation length which plays a central role in the Ginzburg criterion (28) is not large compared to the other microscopic length scale σ. This, incidentally, is one more reason to question the applicability of the Landau theory [26]. Even quite close to the I–N transition the lengths ξ_2 and ξ_4 were quite short and we could not obtain reliable information on their density dependence. At the I–N transition both $g_2(r)$ and $g_4(r)$ become long ranged, as expected. Both $g_2(r)$ and $g_4(r)$ exhibit a monotonic r-dependence, once again quite unlike what is commonly observed in simple molecular fluids. Even though these correlation functions have only been collected over rather limited range of distances we find that the asymptotic behaviour of $g_2(r)$ in the nematic phase agrees quite well with the predicted relation $g_2(r\to\infty)=S^2$ (see table 4). Hence values of $\langle P_2\rangle$ and $\langle P_4\rangle$ may be obtained from the asymptotic values of $g_2(r)$ and $g_4(r)$. In figure 12 we have plotted the MC results for $\langle P_4\rangle$ as a function of $\langle P_2\rangle$. In the same figure we have also indicated the relation between $\langle P_4\rangle$ and $\langle P_2\rangle$ that one would predict if the Maier–Saupe mean-field description were valid. The Maier–Saupe theory assumes that the orientational distribution function is given by :

$$f(\cos\theta)=c\exp(\alpha S P_2(\cos\theta)) \tag{49}$$

with c a normalizing constant and α fixed by the self consistency condition $\langle P_2\rangle=S$ [7]. As can be seen from figure 12 our Monte Carlo data satisfy the Maier–Saupe predictions quite well. This may at first sight seem surprising because the assumptions that are usually involved in any derivation of the Maier–Saupe theory, in particular the one concerning the presence of long-range,

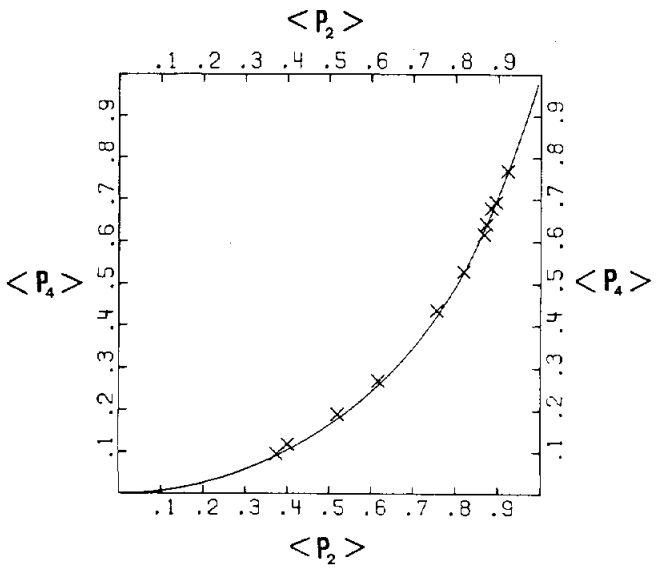

Figure 12. Relation between order parameters $\langle P_2\rangle$ and $\langle P_4\rangle$ for hard-platelet system, compared with Maier–Saupe theory. ×, Monte Carlo data; drawn curve, Maier–Saupe theory.

anisotropic, intermolecular interactions, are certainly not satisfied for the system under consideration. It should be noted however that the functional form given in (49) is the least biased (in the information theoretical sense of the word) distribution function which satisfies the subsidiary condition $\langle P_2 \rangle = S$. Hence it would be unjustified to attach much physical significance to the agreement between our data and the predictions of the Maier–Saupe theory. In fact, we just wish to argue the opposite, namely that success of the Maier–Saupe theory in this respect is in no way an indication that the microscopic picture on which this theory is based is in fact valid. In recent work by Sluckin and Shukla [8] it is shown how a distribution function of the form of (49) may be derived as a special case in a density functional theory of nematics. It is important to note that in the latter theory which, unlike the M–S theory, is in principle applicable to hard platelets, the factor α in (49) has a well defined microscopic meaning. It would be interesting to compare the present results with theoretical predictions based on this theory. Finally we wish to point out the following : for the hard-platelet system (49) is a good approximation, but not exact. One might therefore expect that $f(\cos\theta)$, which was computed during the simulation, contains more information than the average $\langle P_2 \rangle$ and $\langle P_4 \rangle$ discussed above. However, we observed that $f(\cos\theta)$ always fitted well to an expression of the form :

$$f(\cos\theta) = c \exp\left(a_2 P_2(\cos\theta) + a_4 P_4(\cos\theta)\right) \quad \text{with} \quad |a_4| \ll |a_2|.$$

Therefore, all information that we have about $f(\cos\theta)$ is already contained in $\langle P_2 \rangle$ and $\langle P_4 \rangle$.

One of the authors (D.F.) wishes to acknowledge stimulating discussions with Professors Gelbart and Lekkerkerker. Most of the manuscript was written during a visit of D.F. to the Brookhaven National Synchrotron Light Source. We thank Dr. J. P. McTague for the offered hospitality.

Appendix

In this appendix we describe an approximate method to obtain the N-dependence of the different eigenvalues of the Q-tensor (34) :

$$\mathbf{Q} = \frac{1}{N} \sum_i \left[\tfrac{3}{2}(\mathbf{u}_i \,.\, \mathbf{u}_i) - \mathbf{I}/2\right]$$

(where $\mathbf{u}_i = (x_i, y_i, z_i)$ is a unit vector specifying the orientation of molecule i ; we assume cylindrically symmetric molecules).

We consider an idealized model of an orientationally ordered fluid, namely one in which the Q tensors of different particles are uncorrelated, i.e.

$$\langle \mathbf{Q}_i \mathbf{Q}_j \rangle = \langle \mathbf{Q}_i \rangle \langle \mathbf{Q}_j \rangle. \tag{A 1}$$

This situation will occur, for instance, in an non-interacting gas of molecules in a magnetic field. Although in a real liquid crystal (or isotropic fluid) there *are* short range orientational correlation the present analysis is still qualitatively valid in such a system if one reinterprets the $\mathbf{Q}_i$ not as *molecular* Q tensors but as the average Q tensor of a domain of size ξ^3, where ξ is the correlation length of order parameter fluctuations. The eigenvalue equation to be solved is

$$\mathbf{Q} \,.\, \mathbf{v}_n = \lambda_n \mathbf{I} \,.\, \mathbf{v}_n, \tag{A 2}$$

where λ_n is the nth eigenvalue and $\mathbf{v}_n$ the nth eigenvector. It is convenient to study the equivalent problem of finding the eigenvalues of the tensor $\mathbf{M}$:

$$\mathbf{M} \equiv \frac{1}{N} \sum_i \mathbf{u}_i \mathbf{u}_i \tag{A 3}$$

as the eigenvectors of $\mathbf{M}$ are the eigenvectors of $\mathbf{Q}$ and the eigenvalues μ of $\mathbf{M}$ are related to those of $\mathbf{Q}$ by $\mu_n = \frac{2}{3}\lambda_n + 1/3$. The eigenvalue equation for $\mathbf{M}$ then becomes

$$\mathrm{Det}\,(|\mathbf{M} - \mu \mathbf{I}|) = 0 \tag{A 4}$$

or

$$\begin{vmatrix} \frac{1}{N}\sum_i x_i x_i - \mu & \frac{1}{N}\sum_i x_i y_i & \frac{1}{N}\sum_i x_i z_i \\ \frac{1}{N}\sum_i x_i y_i & \frac{1}{N}\sum y_i y_i - \mu & \frac{1}{N}\sum y_i z_i \\ \frac{1}{N}\sum_i x_i z_i & \frac{1}{N}\sum y_i z_i & \frac{1}{N}\sum z_i z_i - \mu \end{vmatrix} = 0$$

or

$$\begin{aligned} -\mu^3 + \mu^2 - \frac{\mu}{N^2}\Bigg(\sum_{i,j} [(x_i x_i y_j y_j - x_i y_i x_j y_j) + (x_i x_i z_j z_j - x_i z_i x_j z_j) \\ + (y_i y_i z_j z_j - y_i z_i y_j z_j)] + \frac{1}{N^3}\Bigg(\sum_{ijk} [(x_i x_i y_j y_j z_k z_k - x_i x_i y_j z_j y_k z_k \\ - y_i y_i z_j x_j z_k x_k - z_i z_i x_j y_j x_k x_k) + 2(x_i y_i y_k z_k z_j x_j)] \Bigg) \\ \equiv -\mu^3 + \mu^2 + c_1 \mu + c_0 = 0 \end{aligned} \tag{A 5}$$

solving this equation yields μ_n as a function of all orientations:

$$\mu_n = f_n(x_1, y_1, z_1, \ldots, x_n, y_n, z_n), \tag{A 6}$$

where f_n is a *non-linear* function of all orientations. To obtain $\langle \mu_n \rangle$ one should average the roots of this non-linear equation. This is in general not possible. We simplify this problem by solving the equation with the *average* coefficients $\langle c \rangle$ and $\langle c_0 \rangle$. Of course, for a non-linear problem this is *not* equivalent to a procedure where the μs are averaged after the equation has been solved. But by checking the dependence of the roots on the values of the coefficients it is easy to verify that the general conclusions obtained below are not affected by the premature averaging. The averaged equation for μ now reads

$$-\mu^3 + \mu^2 - \mu \frac{(N-1)}{N}(\langle x^2 \rangle (\langle x^2 \rangle + 2\langle z^2 \rangle)) + \frac{(N-1)(N-2)}{N^2}\langle x^2 \rangle \langle y^2 \rangle \langle z^2 \rangle, \tag{A 7}$$

where we have used a coordinate system such that the z-axis coincides with the axis of cylindrical symmetry. Moreover, we have used the fact that there is no short range orientational correlation. Using the relation:

$$\left.\begin{aligned} \langle x^2 \rangle = \langle y^2 \rangle = (1 - S)/3 \\ \langle z^2 \rangle = (2S + 1)/3, \end{aligned}\right\} \tag{A 8}$$

and

where S is the nematic order parameter, we obtain the following equation for $\mu = \frac{2}{3}\lambda + 1/3$:

$$\lambda^3 - \tfrac{3}{4}\lambda\left(\frac{1}{N} + S^2(N-1)/N\right) - (S^3/4 + 3(S^2 - S^3)/4N + (1 - 3S^2 + 2S^3)/4N^2) = 0. \qquad \text{(A 9)}$$

This cubic equation can be solved in a closed form.

$$\lambda_n = r\cos\left(\phi_n + (n-1)\frac{2\pi}{3}\right), \quad (n = -1, 0, 1) \qquad \text{(A 10 } a\text{)}$$

with

$$r = \left(\frac{1}{N} + S^2\frac{(N-1)}{N}\right)^{1/2} \qquad \text{(A 10 } b\text{)}$$

and

$$\phi = \tfrac{1}{3}\arccos\left(\frac{(S^3 + 3(S^2 - S^3)/N + (1 - 3S^2 + 2S^3)/N^2)}{(1/N + S^2(N-1)/N)^{3/2}}\right). \qquad \text{(A 10 } c\text{)}$$

Let us consider the isotropic case ($S = 0$) first

$$\left.\begin{aligned} r &= 1/\sqrt{N}, \\ \phi &= \tfrac{1}{3}\arccos(1/\sqrt{N}) \end{aligned}\right\} \qquad \text{(A 11)}$$

for N not too small (say $N > 20$),

$$\arccos(1/\sqrt{N}) \approx \frac{\pi}{2} - 1/\sqrt{N}$$

and hence

$$\phi = \frac{\pi}{6} - \tfrac{1}{3}\sqrt{N}$$

then

$$\left.\begin{aligned} \lambda_0 &= \frac{1}{\sqrt{N}}\cos\left(-\frac{\pi}{2} - \frac{1}{3\sqrt{N}}\right) \approx -\frac{1}{3N}, \\ \lambda_+ &= \frac{1}{\sqrt{N}}\cos\left(\frac{\pi}{6} - \frac{1}{3\sqrt{N}}\right) \approx \frac{1}{\sqrt{N}}\left(\frac{\sqrt{3}}{2} + \frac{1}{6\sqrt{N}}\right), \\ \lambda_- &= \frac{1}{\sqrt{N}}\cos\left(\frac{5\pi}{6} - \frac{1}{3\sqrt{N}}\right) \approx \frac{1}{\sqrt{N}}\left(-\frac{\sqrt{3}}{2} + \frac{1}{6\sqrt{N}}\right) \end{aligned}\right\} \qquad \text{(A 12)}$$

hence : $\lambda_0 = \mathcal{O}(1/N)$ and $\lambda_{\pm}, = \mathcal{O}(1/\sqrt{N})$.

An example of the N-dependence of λ_-, λ_0, λ_+ is shown in figure A 1. Next we go to the case $S \neq 0$. Then :

$$\cos 3\phi = \frac{S^3(1 - 3/N + 2/N^2) + S^2(3/N - 3/N^2) + 1/N^2}{(S^2(1 - 1/N) + 1/N)^{3/2}} \qquad \text{(A 10)}$$

which, to leading order in $1/N$, is equal to :

$$\cos 3\phi \approx 1 - \frac{3}{2N} + \frac{3}{N}\left(\frac{1}{S} - \frac{1}{2S^2}\right). \qquad \text{(A 13)}$$

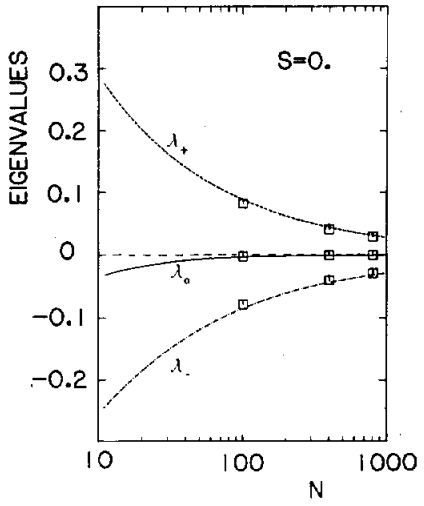

Figure A 1. System size dependence of the three roots of the average Q-tensor, as given by (A 10) for a perfectly isotropic system. In the same figure we have also indicated numerical results for an ideal isotropic gas for $N=100$, 400 and 800 (open squares). Note that the numerical results agree quite well with the (approximate) analytical expressions.

Clearly, for N not too small and S not too small we can expand the cosine to obtain the following equation for ϕ :

$$\phi^2=\frac{1}{3N}-\frac{2}{3N}\left(\frac{1}{S}-\frac{1}{2S^2}\right) \tag{A 14}$$

from which it follows that $\phi=\mathcal{O}(1/\sqrt{N})$. For $S\neq 0$, r is given by :

$$r=(S^2+(1-S^2/N)^{1/2}=S+\frac{(1-S^2)}{2NS}+\mathcal{O}(1/N^2) \tag{A 15}$$

Hence $r=S+\mathcal{O}(1/N)$. If we now look at λ_-, λ_0, λ_+ we obtain

$$\lambda_+=r\cos\phi=(S+\mathcal{O}(1/N))(1-\mathcal{O}(1/N)) \tag{A 16}$$

or

$$\left.\begin{aligned}\lambda_+&=S+\mathcal{O}(1/N)\\ \lambda_0&=r\cos\left(-\frac{2\pi}{3}+\phi\right)=r\left(-\tfrac{1}{2}\cos\phi+\frac{\sqrt{3}}{2}\sin\phi\right)\\ \lambda_-&=r\cos\left(\frac{2\pi}{3}+\phi\right)=r\left(-\tfrac{1}{2}\cos\phi-\frac{\sqrt{3}}{2}\sin\phi\right)\end{aligned}\right\} \tag{A 17}$$

which, to leading order in $1/N$ yields :

$$\lambda_0=S(-\tfrac{1}{2}+c/\sqrt{N}),$$
$$\lambda_-=S(-\tfrac{1}{2}-c/\sqrt{N}).$$

Hence, in the nematic phase, λ_+ yields a better estimate of S. Note that the fact that we find 3 different eigenvalues does not indicate a biaxial phase, because this result was derived *assuming* a uniaxial phase. The *apparent* biaxiality is a system size effect. The dependence of λ_-, λ_0 and λ_+ on S are shown in figure A 2.

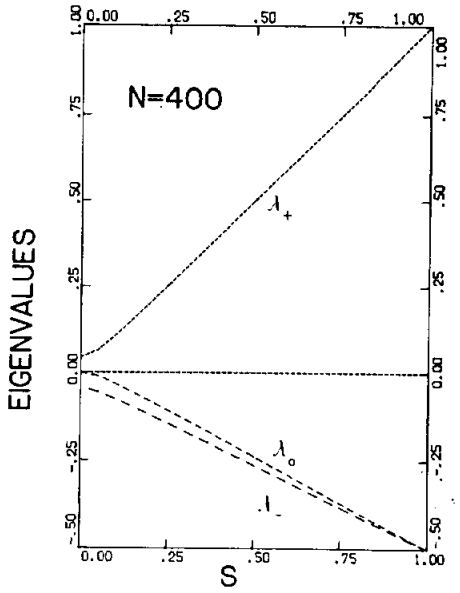

Figure A 2. Relation between the ' real ' (infinite system) order parameter S, and the three roots of the average Q-tensor, as computed using (A 10), for $N=400$. Note that at low values of S, λ_0 approaches zero more rapidly than λ_+ and λ_-. At larger values of S, λ_+ aproaches S.

It is interesting to look at the meaning of fluctuations in λ_0 as studied in this paper. It is illuminating to consider the graphical representation of the eigenvalues shown in figure A 3. The three eigenvalues can be considered as the projection of a triad of vectors of equal length which make angles of 120°

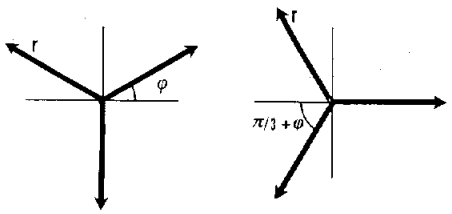

Figure A 3. Graphic representation of the computation of the eigenvalues of the Q-tensor (A 10). The three eigenvalues are given by the projection of the three vectors on the horizontal axis. In the isotropic phase (*a*), $r=\mathcal{O}(1/\sqrt{N})$ while $\phi=\pi/6-\mathcal{O}(1/\sqrt{N})$ In the nematic phase (*b*), $r=S+\mathcal{O}(1/N)$ while $\phi=\mathcal{O}(1/\sqrt{N})$. Fluctuations in the order parameter are caused by fluctuations in both r and ϕ.

with one another. Fluctuations in the order parameters are driven by fluctuations in both the length of the vectors (r) and the angle ϕ. It is important to note that the fluctuations in λ_0 contain both effects i.e. a contribution due to biaxial fluctuations (ϕ) and fluctuations in the size of the order parameter (r). As one approaches the I–N transition, all fluctuations increase in size and ϕ starts to rotate from $\pi/6$ to 0, while r grows from $1/\sqrt{N}$ to S. In the density range where ϕ is halfway between $\pi/6$ and 0 none of the 3 eigenvalues of Q is a good measure for the nematic order parameter.

As stated before, we solved for the eigenvalues λ_-, λ_0, λ_+ after averaging (A 4) over all fluctuations. It is of course interesting to know how seriously the averaging of the non-linear equation affects the predicated average values of λ. To this end we carried out a numerical test on a system of N ideal gas molecules ($N=100$, 400, 800). In figure A 1 we compare the predicted eigenvalues computed from (A 10) with the real average eigenvalues obtained by diagonalizing **Q** for 10^4 independent ideal gas configurations. Clearly, the agreement is quite good.

References

[1] de Gennes, P. G., 1974, *The Physics of Liquid Crystals* (Clarendon Press).
[2] Onsager, L., 1949, *Ann. N.Y. Acad. Sci.*, **51**, 627.
[3] Maier, W., and Saupe, A., 1958, *Z. Naturf.* A, **13**, 564 ; 1959, *Ibid.*, **14**, 882 ; 1960, *Ibid.*, **15**, 287.
[4] Cotter, M. A., 1979, *The Molecular Physics of Liquid Crystals*, edited by G. R. Luckhurst and G. W. Gray (Academic Press), p. 169.
[5] Barboy, B., and Gelbart, W. M., 1980, *J. statist. Phys.*, **22**, 709.
[6] Chandler, D., Weeks, J. D., and Andersen, H. C., 1983, *Science, N.Y.*, **220**, 787.
[7] Luckhurst, G. R., 1979, *The Molecular Physics of Liquid Crystals*, edited by G. R. Luckhurst and G. W. Gray (Academic Press), p. 85.
[8] Sluckin, T. J., and Shukla, P., 1983, *J. Phys.* A, **16**, 1539.
[9] Vieillard-Baron, J., 1974, *Molec. Phys.*, **28**, 809.
[10] Rebertus, D. W., and Sando, K. M., 1977, *J. chem. Phys.*, **67**, 2585. Monson, P. A., and Rigby, M., 1980, *Molec. Phys.*, **39**, 977. Boublik, T., and Nezbeda, I., 1980, *Czech. J. Phys.* B, **30**, 121.
[11] Wood, W. W., 1968, *J. chem. Phys.*, **48**, 415 ; 1970, *Ibid.*, **52**, 729.
[12] McDonald, I. R., 1972, *Molec. Phys.*, **23**, 41.
[13] Widom, B., 1965, *J. chem. Phys.*, **40**, 939.
[14] Valleau, J. P., and Whittington, R. S. G., 1977, *Statistical Mechanics*, edited by B. J. Berne (Plenum Press).
[15] Alder, B. J., Hoover, W. G., and Young, D. A., 1968, *J. chem. Phys.*, **49**, 3688.
[16] Zannoni, C., 1979, *The Molecular Physics of Liquid Crystals*, edited by G. R. Luckhurst and G. W. Gray (Academic Press), p. 51.
[17] Zannoni, C., 1979, *The Molecular Physics in Liquid Crystals*, edited by C. R. Luckhurst and G. W. Gray (Academic Press), p. 200.
[18] Mountain, R. D., and Ruijgrok, T. W., 1977, *Physica* A, **89**, 522.
[19] Ree, F. H., and Hoover, W. G., 1963, *J. chem. Phys.*, **40**, 939.
[20] Eppenga, R., and Frenkel, D. (to be published).
[21] Savithramma, K. L., and Madhusudana, N. V., 1981, *Molec. Crystals liq. Crystals*, **74**, 243.
[22] Frenkel, D., and Eppenga, R., 1982, *Phys. Rev. Lett.*, **49**, 1089.
[23] Lasher, G., 1979, *J. chem. Phys.*, **53**, 4141.
[24] Kayser, R. F., and Raveché, 1979, *Phys. Rev.* A, **17**, 2067.
[25] Buka, A., and de Jeu, W. H., 1982, *J. Phys., Paris*, **43**, 361.
[26] Keyes, P. H., 1978, *Physics Lett.* A, **67**, 132.
[27] Rosenblatt, C., 1983, *Phys. Rev.* A, **27**, 1234.
[28] Landau, L. D., and Lifshitz, E. M., 1958, *Statistical Physics* (Pergamon Press).
[29] Blum, L., and Torruella, A. J., 1972, *J. chem. Phys.*, **56**, 303.

D.~Frenkel and J.~F.~Maguire, Mol.\ Phys.\ {\bf 49}:503 (1983).
R.~Eppenga and D.~Frenkel, Mol.\ Phys.\ {\bf 52}:1303 (1984).
D.~Frenkel, Mol.\ Phys.\ {\bf 54}:145 (1985) B.~M.~Mulder and
D.~Frenkel, Mol.\ Phys.\ {\bf 55}:1193 (1985) D.~Frenkel, Mol.\
Phys.\ {\bf 60}:1 (1987), {\bf 65}:493(1988) C.~Vega and
D.~Frenkel, Mol.\ Phys.\ {\bf 67}:633(1989)